PASJ: Publ. Astron. Soc. Japan , 1–??,

Density and Radius of Dark Matter Halo in the Milky Way Galaxy from a Large-Scale Rotation Curve

Yoshiaki SOFUE
1. Department of Physics, Meisei University, Hino-shi, 191-8506 Tokyo
2. Institute of Astronomy, University of Tokyo, Mitaka, 181-0015 Tokyo
Email:sofue@ioa.s.u-tokyo.ac.jp

(Received 2011draft; accepted 2011draft)

Abstract

A large-scale rotation curve of the Milky Way Galaxy is reconstructed, which covers the area from Galactic Center to Local Group, or from galacto-centric radius $R \sim 0$ kpc to ~ 1 Mpc. The scale radii and masses of the galactic bulge, exponential disk and dark halo are determined by least squares fitting to the rotation curve. The bulge+disk system is shown to have a total mass of only $M_{\rm b}+M_{\rm d} \simeq 3.3\times10^{10}M_\odot$. The Navaro-Frenk-White (NFW) density profile for dark halo, $\rho=\rho_0/([R/h)(1+(R/h)^2)]$ with h and ρ_0 being the scale radius and scale density, respectively, is applied, and the least squares fit yields $h=15.3\pm1.1$ kpc and $\rho_0=(7.18\pm0.90)\times10^{-3}M_\odot$ pc^{-3}. The local value of the dark matter density near the Sun at $R_0=8$ kpc is estimated to be $\rho_0^\odot=(1.08\pm0.17)\times10^{-2}M_\odot$ pc$^{-3}=0.410\pm0.066$ GeV cm^{-3}. The dark matter mass inside the solar circle is $M_{\rm h}(R\leq8$ kpc$)\sim3.9\times10^{10}M_\odot$. The total mass of the entire dark halo inside the supposed boundary of the Galaxy at $R\sim385$ kpc, a half distance to M31, is $M_{\rm h}\sim1.04\times10^{12}M_\odot$. This leads to an upper value of the baryon to dark matter ratio of $(M_{\rm b}+M_{\rm d})/M_{\rm h}\sim3.1\%$. This value is much smaller than the cosmic mean of 19%(=4.6%/24%), implying that the rest 16% ($\sim1.7\times10^{11}M_\odot$) baryons are missing or invisible in our Galaxy.

Key words: galaxies: dark matter — galaxies: structure — galaxies: The Galaxy — galaxies: rotation curve

1. Introduction

The dynamical mass distribution in the Milky Way Galaxy has been obtained by various authors using the rotation curves on the assumption of circular rotation of the galactic disk (see Sofue and Rubin 2001 for review). In our previous work, a large scale rotation curve, called pseudo-rotation curve, has been obtained by combining the current rotation velocity data and radial velocity information of globular clusters and satellite galaxies, and was used to model the dark halo surrounding the Galaxy (Sofue, et al. 2009, Paper I; Sofue 2009, Paper II). While the model fitting to the inner rotation curves was satisfactory, the fitting to the outer rotation curve related to the dark halo was still crude because of the large scatter of kinematical data.

Recently, extensive analyses of galactic rotation curves have been obtained of the dark halo density and representative models (Weber and de Boer 2010; Salucci et al. 2010; and the literature therein). It has been shown that the kinematics of satellite galaxies is crucial for determining the global dark halo models (Paper II).

In this paper we reconstruct a large-scale rotation curve, and discuss the dark halo model of the Galaxy based on the NFW (Navaro, Frenk and White 1996) density profile. During the dark halo fitting, we obtain the least-square fitted parameters of the galactic bulge and disk, as well. Throughout the paper, we adopt a galactocentric distance and circular velocity of the Sun of (R_0,V_0)=(8.0 kpc, 200 km s^{-1}).

2. Observed Rotation Curve and Velocity Dispersion

Figure 1 shows the observed rotation velocities $V(R)$ and galacto-centric radial velocities $V_{\rm GC:obs}$, as reproduced from Paper II, where we compiled kinematical data from the literature and recalculated them for the galactic constants of $(R_0,V_0)=$ (8 kpc, 200 km s^{-1}). The inner data within $R\sim10$ kpc are mostly from the traditional circular velocity measurements of disk objects near the Galactic plane, while some data with large scatter are the galacto-centric velocities of globular clusters. The data from 10 to ∼25 kpc are the mixture of usual circular velocities and galacto-centric radial velocities of globular clusters. Those beyond $R\sim30$ kpc are $V_{\rm GC:obs}$ of distant globular clusters, satellite galaxies, dwarf galaxies, and member galaxies of the Local Group. See Paper II for detail and data references.

A rotation curve is defined by circular velocity $V_{\rm circ}$ in a balance between the centrifugal force and gravity, which is equivalent to the Virial theorem of a circularly rotating disk objects. For non-disk objects like globular clusters and satellites that are moving in statistical and/or random orbits in Virial equilibrium, we define a pseudo-rotation curve as galacto-centric velocity $V_{\rm GC}$ corrected for the freedom of motion of individual objects: its related to the observed galacto-centric velocity $V_{\rm GC:obs}$ as

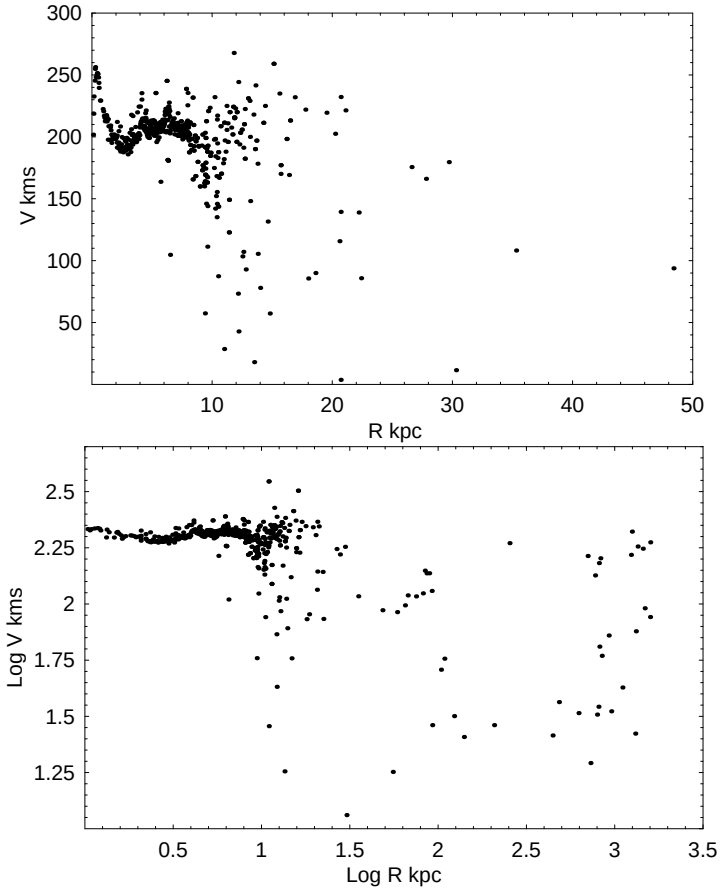

Fig. 1. (a:top) Rotation velocities and galactocentric radial velocities made from the data list in Paper II. (b: bottom) Same, but in logarithmic scaling up to 1 Mpc.

$$V_{\rm GC} = \sqrt{3}\ V_{\rm GC:obs}, \tag{1}$$

where $\sqrt{3}$ is the correction factor for the random three-dimensional directions of freedom 3, when one directional value, e.g. the radial velocity, is observed. We now define the rotation curve as

$$W(R) = V_{\rm circ} \tag{2}$$

for disk objects (HI gas, CO gas, molecular clouds, HII regions, OB stars, and red giants in the disk), and

$$W(R) = V_{\rm GC} = \sqrt{3} V_{\rm GC:obs} \tag{3}$$

for non-disk objects (globular clusters, satellites, dwarf galaxies, Local Group galaxies).

In order to obtain a smooth rotation curve, we apply a running mean of the observed values in figure 1. We define a rotation velocity at R_i as

$$V(R_i) = \frac{\Sigma_{j=i-N}^{i+N} W(R_j)}{2N+1}, \tag{4}$$

where $2N+1$ is the number of used data points around $R = R_i$, which is taken every N steps in the data list in the order of increasing radius. In the present paper we take $N = 5$, so that the data are running averaged every $N = 5$ points using their neighboring $2N+1 = 11$ objects. We also calculate the velocity dispersion by

$$\sigma(R_i) = \sqrt{\frac{\Sigma_{j=i-N}^{i+N} [V(R_j) - W(R_i)]^2}{(2N+1)-1}} \tag{5}$$

Figure 2 shows the obtained rotation curve and 5 . Note that the observational errors of individual data points are much less than the scatter in this plot, e.g. $\sigma(R_i)$ is much larger than the observational error. In this meaning $\sigma(R_i)$ represents the real velocity dispersion of the objects in each averaging bin. Table 2 lists the obtained rotation velocities used for figure 2.

3. Fitting Model

We assume that the rotation curve is composed of a bulge, disk, and dark halo components, and is calculated by

$$V(R)^2 = V_{\rm b}(R)^2 + V_{\rm d}(R)^2 + V_{\rm h}(R)^2, \tag{6}$$

where $V(R)$, $V_{\rm b}(R)$, $V_{\rm d}(R)$, and $V_{\rm h}(R)$ are the circular rotation velocity at galactocentric distance R, the corresponding circular velocity due to the bulge, disk and dark halo, respectively. Using the newly constructed rotation curve in figure 2, we construct a model rotation curve using the least square fitting.

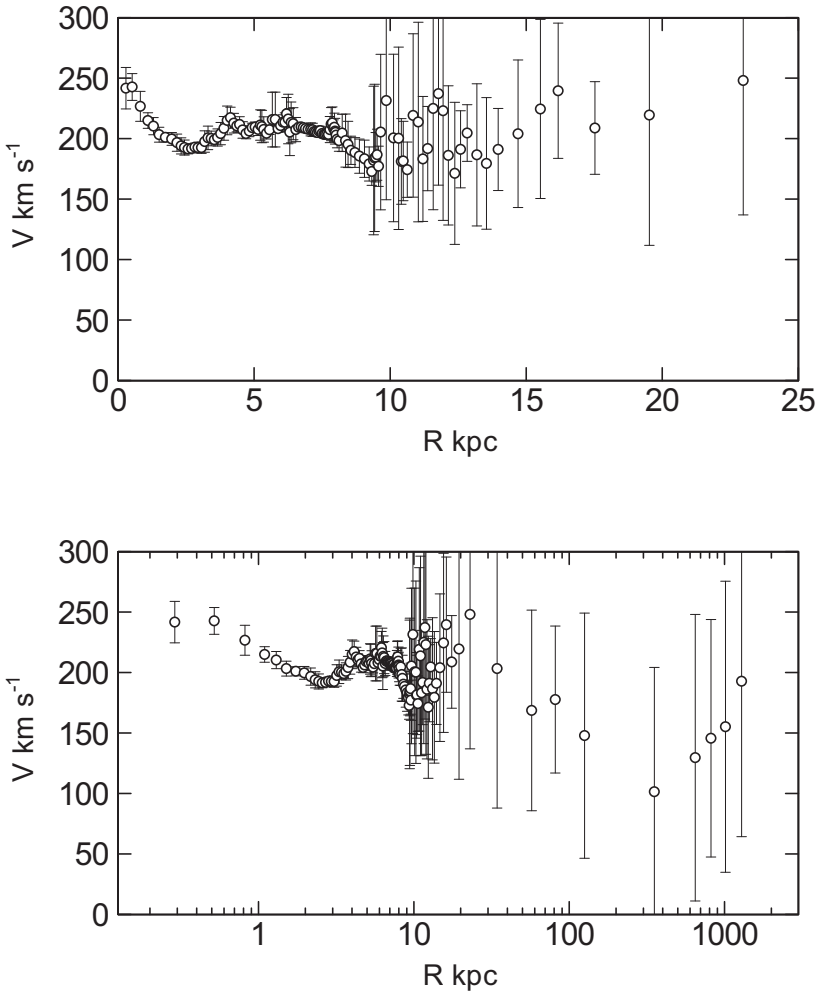

Fig. 2. Rotation curve $V(R_i)$ of the Galaxy obtained by running mean of $11 = 2 \times 5 + 1$ neighboring data at every 5 data points in the order of increasing radius. The bars indicate least-square fit dispersion in each bin. Top panel shows the data within 25 kpc, and the bottom within the Local Group. Note the abscissa in the bottom figure is logarithmic.

3.1. Bulge

The bulge is assumed to have a Plummer type potential represented by

$$\phi = \frac{GM_{\rm b}}{\sqrt{R^2 + a_{\rm b}^2}} \tag{7}$$

yielding circular velocity as

$$V(R) = \sqrt{\frac{GM_{\rm b}}{a_{\rm b}}} \left(\frac{R}{a_{\rm b}}\right) \left\{1 + \left(\frac{R}{a_{\rm b}}\right)^2\right\}^{-3/4}, \tag{8}$$

where G is the gravitational constant, and $M_{\rm b}$ and $a_{\rm b}$ are the masses and scale radii of the bulge.

A better expression for the bulge's surface density distribution is the de Vaucouleurs law (de Vaucouleurs 1958; Paper I). However, calculation of its circular velocity is not straightforward, and we may approximate the density profile by the Plummer law, which is sufficiently accurate for the present purpose to study the outermost behavior related to the dark halo.

3.2. Disk

The galactic disk is approximated by an exponential disk, whose surface mass density is expressed as

$$\Sigma_{\rm d}(R) = \Sigma_0 \exp\left(-\frac{R}{a_{\rm d}}\right), \tag{9}$$

where Σ_0 is the central value and $a_{\rm d}$ is the scale radius. The total mass of the exponential disk is given by

$$M_{\rm d} = 2\pi\Sigma_0 a_{\rm d}^2. \tag{10}$$

The rotation curve for a thin exponential disk is expressed by

$$V_{\rm d} = \sqrt{4\pi G\Sigma_0 a_{\rm d} \mathscr{B}(y)} = \sqrt{\frac{2GM_{\rm d}}{a_{\rm d}} \mathscr{B}(y)}, \tag{11}$$

Table 1. Rotation Curve of the Galaxy†

Radius (kpc)	Velocity (km s^{-1})	Velo. Dispersion (km s^{-1})
0.29	241.68	17.15
0.52	242.67	11.06
0.82	226.67	12.34
1.10	214.93	6.44
1.30	210.32	7.12
1.51	203.26	6.14
1.74	201.01	3.76
1.97	199.71	5.23
2.17	196.65	7.07
2.32	193.97	6.63
2.44	192.61	6.22
2.57	191.40	4.05
2.70	191.84	3.76
2.82	192.93	3.29
2.94	192.51	3.70
3.06	192.54	4.76
3.19	197.59	8.86
3.30	200.61	9.73
3.42	200.16	6.08
3.54	199.11	3.43
3.65	200.92	7.10
3.77	204.13	9.23
3.89	208.48	9.79
4.01	215.06	11.90
4.13	217.24	8.67
4.25	212.75	8.18
4.36	210.44	4.87
4.47	211.66	6.42
4.58	207.17	6.82
4.70	204.11	4.28
4.82	206.15	4.52
4.93	209.06	3.71
5.04	209.52	4.25
5.15	207.55	5.04
5.23	211.21	12.58
5.29	209.96	13.40
5.35	207.53	10.47
5.46	204.40	4.75
5.57	207.26	3.85
5.67	215.69	22.63
5.78	215.79	22.64
5.88	208.23	2.90
5.97	210.75	5.28

† Ascii data for this table is available from URL http://www.ioa.s.u-tokyo.ac.jp/šofue/htdocs/dh11/

Table 1. (continued)

Radius (kpc)	Velocity (km s^{-1})	Velo. Disp (km s^{-1})
6.06	213.56	6.12
6.13	213.48	7.74
6.19	220.51	13.49
6.25	216.21	20.47
6.31	205.33	19.41
6.36	213.35	16.86
6.44	212.29	13.26
6.53	207.48	10.00
6.63	209.43	1.79
6.73	209.67	1.68
6.81	209.05	3.27
6.89	208.27	3.46
6.98	207.59	2.77
7.08	207.63	5.43
7.15	207.29	5.40
7.20	205.80	3.17
7.25	205.39	2.77
7.32	204.97	2.48
7.38	206.16	4.09
7.43	206.58	3.64
7.50	204.22	3.06
7.56	203.44	2.95
7.61	203.58	2.31
7.67	203.82	3.32
7.73	203.45	3.40
7.79	207.44	10.80
7.83	211.94	13.68
7.87	212.88	13.33
7.92	208.39	7.09
7.95	209.44	11.60
7.97	206.15	10.61
7.99	205.19	4.75
8.01	202.87	4.89
8.05	199.40	6.98
8.12	198.32	8.75
8.24	204.65	15.38
8.36	198.36	21.93
8.45	195.20	19.12
8.56	190.32	11.68
8.71	188.50	12.28
8.87	185.50	14.11
9.05	183.34	15.41
9.23	179.03	14.10
9.33	172.79	11.38
9.39	181.94	61.43
9.43	184.03	60.87
9.47	184.63	20.42
9.52	186.66	21.11
9.58	177.12	16.64
9.65	205.35	64.30
9.86	231.41	81.98

Table 1. (continued)

Radius (kpc)	Velocity (km s^{-1})	Velo. Disp (km s^{-1})
10.12	200.57	69.26
10.31	200.24	75.42
10.41	181.08	35.40
10.48	181.50	32.80
10.63	174.31	22.83
10.84	219.11	67.55
11.03	213.71	82.47
11.20	183.18	51.69
11.38	191.73	34.85
11.58	224.97	83.74
11.78	237.12	75.61
11.94	223.05	90.62
12.14	186.12	57.58
12.37	171.30	58.76
12.59	191.17	31.90
12.83	204.65	23.42
13.18	186.57	58.77
13.54	179.47	54.40
13.97	191.01	33.91
14.70	204.01	60.99
15.52	224.50	74.06
16.18	239.57	55.88
17.52	208.75	38.33
19.53	219.46	107.74
22.98	248.05	111.14
34.35	203.25	115.29
57.36	168.65	82.96
81.39	177.65	60.80
125.49	147.79	101.38
353.29	101.45	102.82
647.55	129.54	118.48
817.71	145.65	98.18
1012.54	155.16	120.30
1287.15	192.82	128.58

where

$$\mathscr{B}(y) = y^2[I_0(y)K_0(y) - I_1(y)K_1(y)] \tag{12}$$

with $y = R/(2R_{\rm d})$, and I_i and K_i being the modified Bessel functions (Freeman 1970).

3.3. Dark Halo

For the dark halo, three mass models have been so far proposed: the semi-isothermal spherical distribution (Begeman et al. 1991), NFW (Navarro, Frenk and White 1996), and Burkert (1996) models. In Paper II, we have shown that the isothermal model may be not a good approximation to the observed rotation curve, and showed that the NFW and Burkert models may better fit the observations. Since the NFW and Burkert profiles are essentially the same, except for the very inner region where the contribution from the dark halo component is negligible, we here adopt the NFW profile. It is expressed as

$$\rho(R) = \rho_0 \left[\frac{R}{h} \left\{ 1 + \left(\frac{R}{h} \right)^2 \right\} \right]^{-1}, \tag{13}$$

where ρ_0 is the representative (scale) density at $R = 0.682h$, or $\rho_0 = \rho(0.682h)$, and h is the scale radius (core radius) of the dark halo.

The enclosed mass within a radius R is given by

$$M_{\rm h}(R) = 4\pi \int_0^R \rho(x) x^2 dx = 2\pi\rho_0 h^3 \ln\left\{ 1 + \left(\frac{R}{h} \right)^2 \right\}. \tag{14}$$

The corresponding circular rotation velocity is given by

$$V_{\rm h}(R) = \sqrt{\frac{GM_{\rm h}(R)}{R}} = \sqrt{\frac{2\pi\rho_0 h^3}{R} \ln\left\{ 1 + \left(\frac{R}{h} \right)^2 \right\}}. \tag{15}$$

4. The Least-Square Fitting

We divide the data of running-averaged rotation velocities shown in table 2 and figure 2 into two parts: inner data set for $R \leq 10$ kpc, and outer set at $10 < R \leq 400$ kpc. The outermost boundary for the fitting is so chosen that it represents the gravitational boundary between the Galaxy and M31, or about a half distance, 385 kpc, to M31 at 790 kpc, as discussed in Paper II.

We find the best fit values for M_i and a_i for the bulge and disk by the least square method using the inner data at $R \leq 10$ kpc, where the dark halo parameters are given as provisional initial values. Using the fitted bulge and disk parameters, we then find the best fit values of ρ_0 and h for the dark halo using the outer data at $10 < R \leq 400$ kpc. The thus found ρ_0 and h are again used in finding the disk and bulge parameters, which is further used to find the halo parameters. This procedure is repeated several times until the fitted results reach sufficiently stable values. Below, we describe the procedure in more details.

We define ξ as

$$\xi = \sqrt{\frac{\Sigma[V_{\rm obs}(R_i) - V(R_i)]^2}{K - 1}}, \tag{16}$$

where $V_{\rm obs}$ is the observed value plotted in figure 5, and K is the number of used data points. Therefore, K is the number of plotted points at $R \leq 10$ kpc for the fitting of the bulge and disk, while it is the number of points at $10 < R \leq 400$ kpc for the dark halo.

We here regard all the plotted points to have the same weight for the following reason: Since the plotted values in figure 2 are the running means of the observations, the bars in the plot are not measurement errors. Particularly, the outer data points include real velocity dispersion, while we are interested in the mean values. In order to discuss the dark halo using the outermost velocity information, it is not practical to apply such weighting that is proportional to the inverse of the square of measurement error bars, which should give a very small weighting to the outermost rotation curve.

Since the number of parameters to be determined is six (a_1, M_1, a_2, M_2, ρ_0, and h), it is not practical to obtain the best fit by one time iteration, we apply a step-by-step iteration as the following.

We first find values of a_1 and M_1 that minimizes ξ for an appropriately assumed initial values of a_2, M_2, ρ_0 and h, using the inner data set at $R \leq 10$ kpc. We calculate ξ by changing a_1 and M_1 at small steps by about hundred times each. Among the various a_1 and M_1 we can fix the best fit values that give minimum ξ. Thus found a_1 and M_1 is used to find the best fit a_2 and M_2 for the same assumed ρ_0 and h. Then, the best fit a_1, a_2, M_1 and M_2 are used to find the best fit h and ρ_0 by the same procedure using the outer data set at $10 < R \leq 400$ kpc. We thus obtain the first step iteration, each of the best fit value is found by about 100 times search for minimum ξ around its associated parameter. The initially assumed values are now replaced by the thus obtained first step best fit values to calculate the second step best fit parameters. This step-by-step iteration is repeated several times to reach a stable minimum ξ value.

By this step-by-step iteration, we have obtained a unique set of the best-fit values of the scale radii and masses of the bulge disk, and dark halo. Figure 3 shows the variations of ξ as a function of each parameter around its best fit value. The error of a fitted parameter is calculated as the range in the fitted value allowing for 10% increase in ξ around its minimum value, or about 20% increase in ξ^2.

5. The Best-Fit Parameters and Rotation Curve

Table 5 shows the best-fit parameters for individual mass components of the Galaxy.

5.1. Radii and Masses of the Bulge and Disk

The scale radius $a_{\rm b} = 244$ pc and mass $M_{\rm b} = 0.860 \times 10^{10} M_\odot$ for the bulge are in good agreement with those obtained so far in the literature. The disk scale radius $a_{\rm d} = 1.88$ kpc is slightly smaller than that often used in the literature of about 3-4 kpc. The disk mass of $M_{\rm d} = 2.43 \times 10^{10} M_\odot$ is almost a half of that often quoted in the literature. The scatter of data around the fitted model is

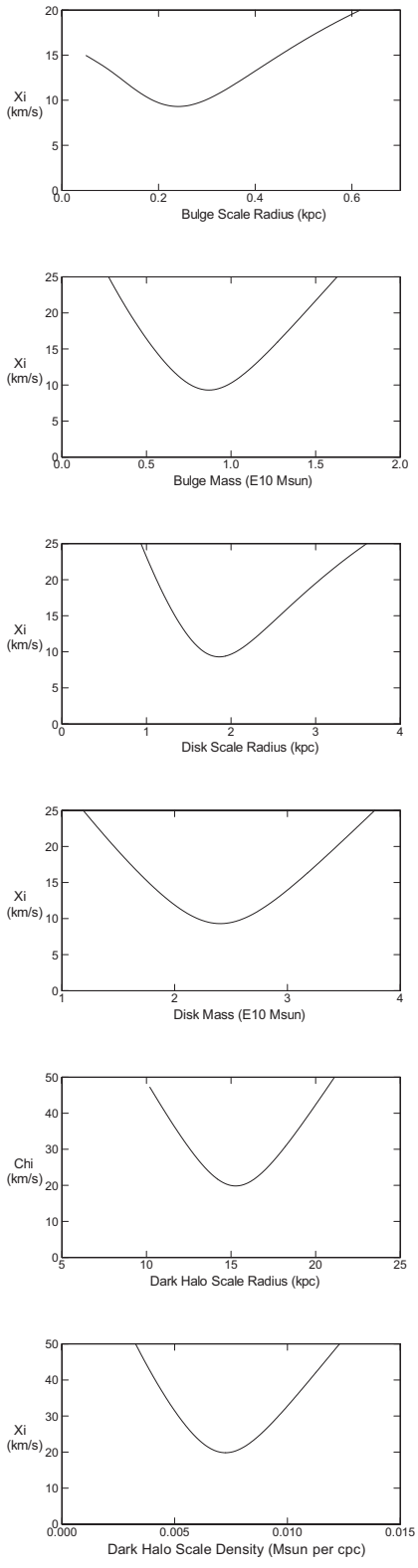

Fig. 3. Variation of ξ as a function of the associated parameter for bulge, disk and dark halo with the other best fit parameters being fixed.

Table 2. Best-fit parameters for the mass components of the Galaxy

Mass component	Mass; Density	Scale Radius	Dispersion ξ
Bulge	$M_{\rm b} = (0.860 \pm 0.120) \times 10^{10} M_\odot$	$a_{\rm b} = 0.244 \pm 0.020$ kpc	9.3 km s^{-1}
Disk	$M_{\rm d} = (2.43 \pm 0.25) \times 10^{10} M_\odot$	$a_{\rm d} = 1.98 \pm 0.20$ kpc	9.3 km s^{-1}
Dark Halo	$\rho_0 = (7.18 \pm 0.90) \times 10^{-3} M_\odot {\rm pc}^{-3}$ $= 0.276 \pm 0.034$ GeV cm^{-3}	$h = 15.3 \pm 1.1$ kpc	19.8 km s^{-1}
Local DM density† * at Sun ($R = 8$ kpc)	$\rho_0^\odot = (1.08 \pm 0.17) \times 10^{-2} M_\odot {\rm pc}^{-3}$ $= 0.410 \pm 0.066$ GeV cm^{-3}		
Bulge+Disk Mass‡	$M_{\rm b} + M_{\rm d} = (3.29 \pm 0.28) \times 10^{10} M_\odot$		
DM Mass *	$M_{\rm h}(R \le 8{\rm kpc}) = (3.91 \pm 0.82) \times 10^{10} M_\odot$ $M_{\rm h}(R \le h) = (1.12 \pm 0.28) \times 10^{11} M_\odot$ $M_{\rm h}(R \le 20{\rm kpc}) = (1.61 \pm 0.40) \times 10^{11} M_\odot$ $M_{\rm h}(R \le 385{\rm kpc}) = (1.04 \pm 0.26) \times 10^{12} M_\odot$		

‡ Upper limit to the baryonic mass.
† Conversion relation from mass to energy density is 1 $M_\odot {\rm pc}^{-3} = 37.983 {\rm GeV cm}^{-3}$.
∗ Errors were calculated by considering the propagation of individual errors $\delta\rho_0$ and δh in the 3rd raw through equations 13 and 14.

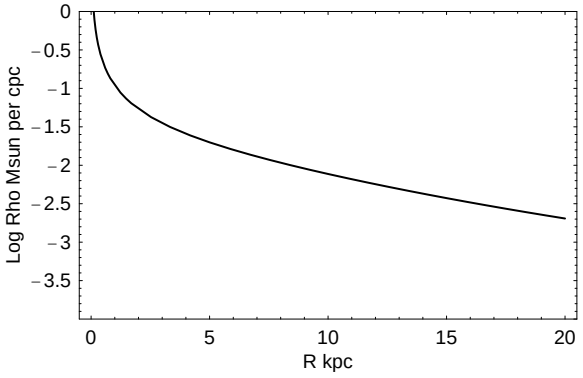

Fig. 4. NFW density profile of the dark matter halo of the Milky Way Galaxy plotted against the galacto-centric radius R.

$\xi = 9.3$ km s^{-1}.

These smaller values for the disk is due to the fact that the dark halo contribution is larger than that expected from the previous studies. In fact, the fitting was obtained by seriously counting the dark halo mass that fills the whole Galaxy up to its gravitational boundary at $R \sim 400$ kpc. Also, in order to yield the same circular velocity at $R = 2 - 8$ kpc, the exponential disk requires 20 to 30% smaller mass than that required by other potential models such as of Plummer type or spherical mass models.

5.2. Dark halo radius and density

The best fit scale radius of the dark halo was obtained to be

$$h = 15.3 \pm 1.1 \text{ kpc}, \tag{17}$$

and the scale (representative) density

$$\rho_0 = (7.18 \pm 0.90) \times 10^{-3} M_\odot {\rm pc}^{-3} \tag{18}$$

or

$$\rho_0 = 0.276 \pm 0.034 \text{ GeV cm}^{-3}, \tag{19}$$

which give the least ξ value of

$$\xi = 19.8 \text{ km s}^{-1} \tag{20}$$

Figure 4 shows the obtained NFW profile for the best fit parameters. The local value near the Sun at $R = 8$ kpc is estimated to be

$$\rho_0^\odot = (1.08 \pm 0.17) \times 10^{-2} M_\odot \text{ pc}^{-3}, \tag{21}$$

or

$$\rho_0^\odot = 0.410 \pm 0.066 \text{ GeV cm}^{-3}. \tag{22}$$

5.3. The Best-Fit Rotation Curve

Figure 5 shows the best-fit rotation curve and those for individual components of bulge, disk and dark halo, calculated by using the parameters in table 5. The calculated rotation curve well reproduces the observed data, except for the wavy and bumpy behaviors, which are attributable

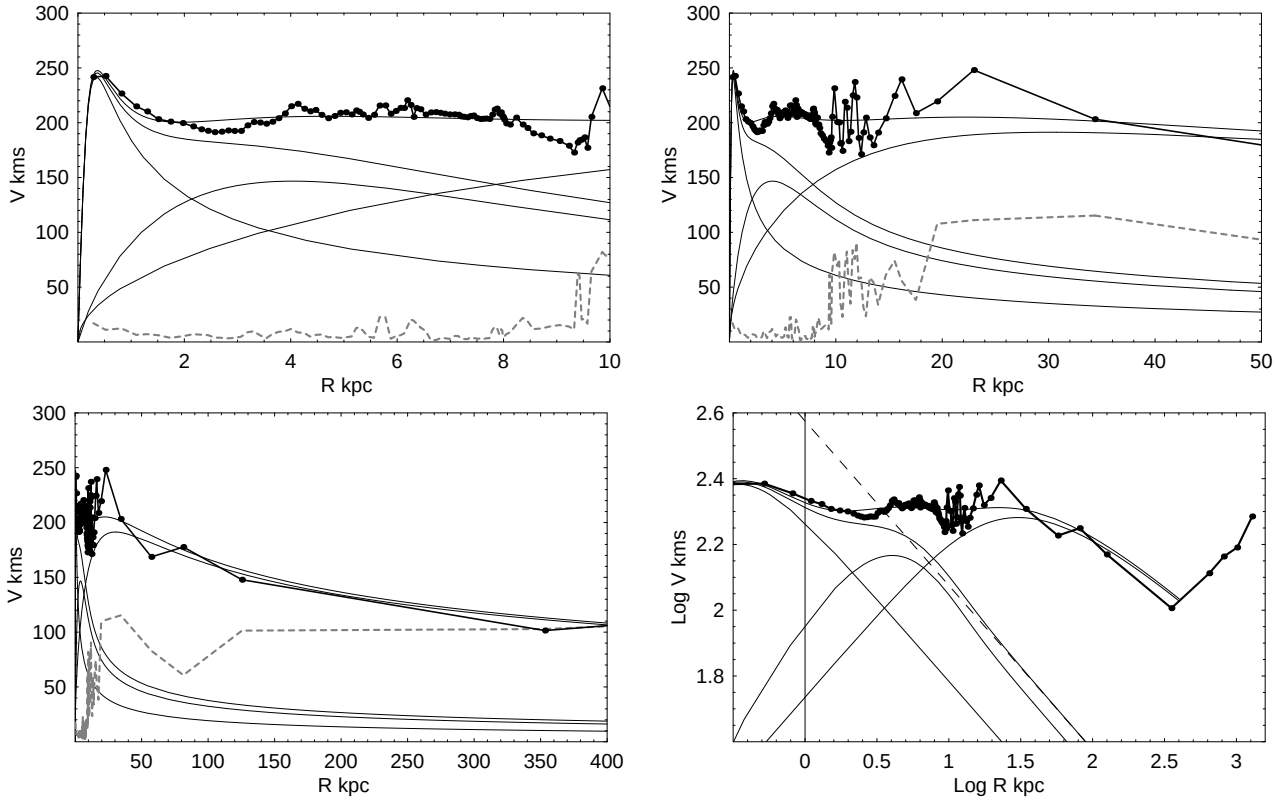

Fig. 5. Observed rotation velocities $V(R_i)$ are shown by filled circles connected by thick lines, and velocity dispersion $\sigma(R_i)$ is shown by grey-dashed line. Best-fit model to the data are shown by thin lines for bulge, disk, bulge+disk dark halo, and total rotation curve, from bottom to top at $R = 10$ kpc. The four panels show the same but for different radius ranges. The last panel shows the same in logarithmic scaling. The dashed straight line in the last figure represents Keplerian law corresponding to the total mass of the bulge and disk components.

to local rings and/or arm structures as discussed in Paper I.

6. Discussion

We have constructed a rotation curve of the Milky Way Galaxy using the data compiled in Paper I, which covers a wide area from the Galactic Center to the outermost boundary of the Milky Way at $R \sim 400$ kpc. By the least-squares fitting to the observed rotation curve, the parameters of the three mass components, the bulge, exponential disk and dark halo with NFW profile have been determined. The result is listed in table 5.

The fitting was obtained more naturally compared to our earlier works (Paper I, II), where one additional condition was given so that the contributions by the disk and dark halo were equal at an assumed critical radius $R = R_{\rm c} \sim 15$ kpc. Removing this condition, the present least-square fitting more honestly reflects the observations, and the result is more reliable. As a consequence, the critical radius was found to be at as inner as $R{\rm c} = 7.8$ kpc.

The parameters for the bulge is not much different from the current works, because the corresponding rotation profile at $R \sim 1$ kpc has a steep peak and the least square fitting is more independent and effective compared to the fit to other extended components like the disk and halo.

The exponential disk was found to have smaller mass and scale radius than the usual values. This indicates a smaller total mass of the bulge and disk system, $M_{\rm b} + M_{\rm d} = 3.3 \times 10^{10} M_\odot$, about a half of that so far quoted. This smaller value is due to a greater contribution from the dark matter: the mass involved inside the solar circle is shared more by the dark matter than the disk+bulge components, as represented by the small critical radius $R_{\rm c} = 7.8$ kpc. In fact, the total mass of dark matter included in the Solar circle sphere is calculated to be $M_{\rm h}(R \le R_0) \sim 3.91 \times 10^{10} M_\odot$, larger than the mass of the disk and bulge.

We may here confirm that the total mass of the bulge, disk and dark halo within the solar circle is comparable to a simple spherical mass estimate for $V_0 = 200$ km s^{-1}at $R_0 = 8$ kpc,

$$M_{\rm G} = \frac{R_0 V_0^2}{G} = 7.44 \times 10^{10} M_\odot, \tag{23}$$

as

$$M_{\rm b} + M_{\rm d} + M_{\rm h}(R \le R_0) = 7.2 \times 10^{10} M_\odot \simeq M_{\rm G}. \tag{24}$$

The local value of the dark matter density in the Solar neighborhood as derived from the present analysis, $\rho_0^\odot = 0.410 \pm 0.066$ GeV cm^{-3}, is consistent with the recently published values 0.43 ± 0.10 GeV cm^{-3}by Salucci et al.

(2010), and 0.2 - 0.4 GeV cm^{-3}by Weber and de Boer (2010).

The total Galaxy mass involved in the supposed boundary of the Galaxy at 385 kpc, a half distance to M31, is $M_{\rm h}(R \leq 385) \sim 1.04 \times 10^{12} M_\odot$. As discussed in Paper II, this mass is not sufficient to gravitationally stabilize the Galaxy+M31 system, and therefore the two galaxies may be embedded in a larger-scale dark matter system properly constructing the Local Group.

If we compare the total dark matter mass with the bulge+disk mass, which is an upper limit of galactic baryonic mass, we obtain an upper value to the baryon-to-dark matter ratio in the entire Galaxy on the order of

$$(M_{\rm b} + M_{\rm d})/M_{\rm h} \sim 3.1\%. \tag{25}$$

This ratio is much smaller than the WMAP's cosmic mean value of 4.6%/24%=19%. Hence, the rest 16% of the baryonic mass of the Galaxy is missing, or baryons of at least $\sim 1.7 \times 10^{11} M_\odot$ are still invisible, neither as gas nor stars. Thus, the Milky Way Galaxy is much more dark matter dominant than so far considered, and the huge amount of missing baryons in our Galaxy remains as a mystery.

References

Begeman KG, Broeils AH, Sanders RH. 1991. MNRAS 249:523
Burkert, A., 1995, ApJ, 447, L25
de Vaucouleurs, G. 1958, ApJ, 128, 465
Freeman, K. C. 1970, ApJ, 160, 811
Navarro, J. F., Frenk, C. S., White, S. D. M., 1996, ApJ, 462, 563
Salucci, P., Nesti, F., Gentile, G., Martins, C. F. 2010 AA 523,83.
Sofue, Y., Honma, M., Omodaka, T. 2009 PASJ, 61, 227 (Paper I).
Sofue, Y. 2009 PASJ 61, 153 (Paper II).
Sofue, Y., Rubin, V.C. 2001 ARAA 39, 137
Weber, M. and de Boer, W. 2010 AA 509, 25.